Experimental characterisation of Eckalite-1 Australian kaolin

Lucian Canales-Brenlla[1*], *Frederik* Koch[1], *Merita* Tafili[1], *Luis F.* Prada-Sarmiento[2], and *Torsten* Wichtmann[1]

[1] Faculty of Civil and Environmental Engineering, Ruhr-University Bochum, Bochum, Germany
[2] Department of Civil and Architectural Engineering, Aarhus University, Aarhus, Denmark

1 Introduction

This study presents the findings of an experimental investigation of Eckalite-1 Australian kaolin clay (A-kaolin), comprising its classification and stress-strain behaviour under undrained monotonic and cyclic loading. In the cyclic tests, the influence of the stress amplitude, consolidation stress, displacement rate, and inherent anisotropy is investigated with selected tests to illustrate the general trends observed. As is well known, experimental databases are essential to properly understand the material behaviour and to develop numerical models that can accurately predict the soil response. The A-kaolin tested in this study is classified as highly-plastic and its mechanical behaviour is compared to experiments of a less plastic kaolin, namely Karlsruhe kaolin (K-kaolin) presented in [1]. In this regard, the influence of viscous effects, i.e., effect of loading rate on the cumulative effects, is presumed to be larger. The experimental results were used to evaluate the ability of the anisotropic visco-hypoplastic (AVHP) model [2] to capture key features of the observed behaviour.

2 Test material and laboratory tests

The tested kaolin, A-kaolin, is commercially available from the producer Imerys (Imerys Minerals Australia Pty Ltd). In particular, the designation Eckalite-1 kaolin is described as a high-quality, water washed clay with controlled color and particle size distribution. Standard classification tests have been performed at Ruhr-University Bochum (RUB), obtaining a liquid limit of $w_L = 62.4$ %, plastic limit $w_P = 38.9$ % and plasticity index of $I_p = 23.5$ %. On the other hand, K-kaolin shows a lower plasticity ($I_p = 12.2$ %) [1]. According to their position on the Casagrande's diagram, A-kaolin and K-kaolin are classified as high-plastic and medium-plastic silts, respectively (Figure 1a). The grain density of the solid soils ρ_s for A-kaolin was determined according to DIN EN ISO 17892-3 and corresponds to a specific gravity $G_s \approx 2.60$. A summary of the index properties for both kaolin clays is given in Table 1. Moreover, the grain size distribution curve obtained from a sedimentation analysis shows that A-kaolin is finer-grained than K-kaolin (Figure 1b).

To perform the triaxial tests, reconstituted samples out of a slurry prepared from dry kaolin powder mixed with demineralized water at a high-water content (min. $w/w_L = 2.5$) were used. A maximum vertical stress during pre-consolidation of $\sigma_{1,precons} = 100$ kPa was applied to all tested samples. Furthermore, a sample geometry with a diameter d and height h of 5 cm, i.e., a height-to-diameter ratio $h/d = 1$, was chosen to allow faster consolidation and homogenization times. In previous studies by the last author, samples tested with a $h/d = 1$ and $h/d = 2$ were found to deliver closely matching results under undrained cyclic loading and hence the undrained cyclic strength was found not to be dependent on the sample geometry [3]. Smeared end plates consisting of a thin layer of grease and a latex membrane were used in all tests. Consolidated undrained (CU) monotonic and cyclic triaxial tests were carried out to evaluate the mechanical behavior of A-kaolin. In all cases, the criteria followed for the chosen loading rate was a sufficiently low displacement rate $\dot{s}$ to ensure a homogenous field of pore water pressure within the samples. Furthermore, all samples were isotropically consolidated to the initial mean effective stress p'_0 after being water saturated with a back-pressure of 500 kPa. Figure 1c-f, presents the results of undrained monotonic tests for two different mean effective stresses, namely $p'_0 = 100$ and 300 kPa. The effective stress paths in the $p' - q$ plane, where $p' = (\sigma'_1 + 2\sigma'_3)/3$ and the deviatoric stress $q = \sigma'_1 - \sigma'_3$, show a predominant contractive behavior (Figure 1d). Also, the slope of the failure surface seems to be better described with a curvature, similar as reported for K-kaolin in [1]. For the purpose of the numerical simulations with the AVHP model, a value of $M_c = 1.00$ and 1.12 has been adopted for K-kaolin and A-kaolin, respectively. The stress-strain relationship $q(\varepsilon_1)$ curves, shown in Figure 1f, are reported only until the onset of shear bands usually observed during the tests (at $\varepsilon_1 \approx 15$ %), therefore no claim of a full critical state can be made.

Table 1. Index properties of the kaolin clays compared in this study: K-kaolin [a] and A-kaolin.

Material	w_L (%)	w_P (%)	I_P (%)	ρ_s (g/cm^3)
Karlsruhe kaolin clay (K-kaolin) [a]	47.2	35.0	12.2	2.675
Eckalite-1 Australian kaolin clay (A-kaolin)	62.4	38.9	23.5	2.598

[a] From Wichtmann and Triantafyllidis [1].

* Corresponding author: lucian.canalesbrenlla@rub.de

In the CU cyclic triaxial tests, the stress cycles were applied at a constant displacement rate $\dot{s}$ in which the loading direction was changed once the minimum and maximum prescribed values of deviatoric stress q were met. In this regard, the cyclic loading was stopped once the failure criterion, defined as axial strain $|\varepsilon_1 = 10\ \%|$, was reached. For all tests, isotropic consolidation until the initial mean effective stress p'_0 and an overconsolidation ratio (OCR) of 1 has been considered. Representative results of a CU cyclic test for both materials under the same test conditions are shown in Figure 2, with A-kaolin showing a lower number of cycles to failure N_f. As shown in Figure 2c, d, both materials reached the failure criteria at larger strains, as can be expected from samples isotropically consolidated. Notably, the soil response in the $p' - q$ plane for A-kaolin shows a higher initial loading stiffness with a distinctive effective stress path during the first cycle. The shape of the final loops in the $p' - q$ plane (eight-shaped effective stress paths) and in the $\varepsilon_1 - q$ plane can be considered similar between both kaolin clays. Further CU cyclic tests results on A-kaolin with variation of the deviatoric stress amplitude q^{ampl} (Figure 3b, f, j), the initial mean effective stress p'_0 (Figure 3c, g, k), and the loading rate $\dot{s}$ (Figure 3d, h, l) are discussed. Taking as reference the test results in Figure 3a, e, i, the rate of pore water pressure increases with increasing q^{ampl} and p'_0. For the latter case, differing with the observed trend reported for K-kaolin in [1,3]. In regard to the influence of the loading rate, there is no indication that N_f decreases with decreasing $\dot{s}$, yet the shape of the final loops seems to be influenced to some extent. Acknowledging the number of tests and natural scatter, e.g., variations of the initial void ratio e_0, additional tests are required to confirm the observations made.

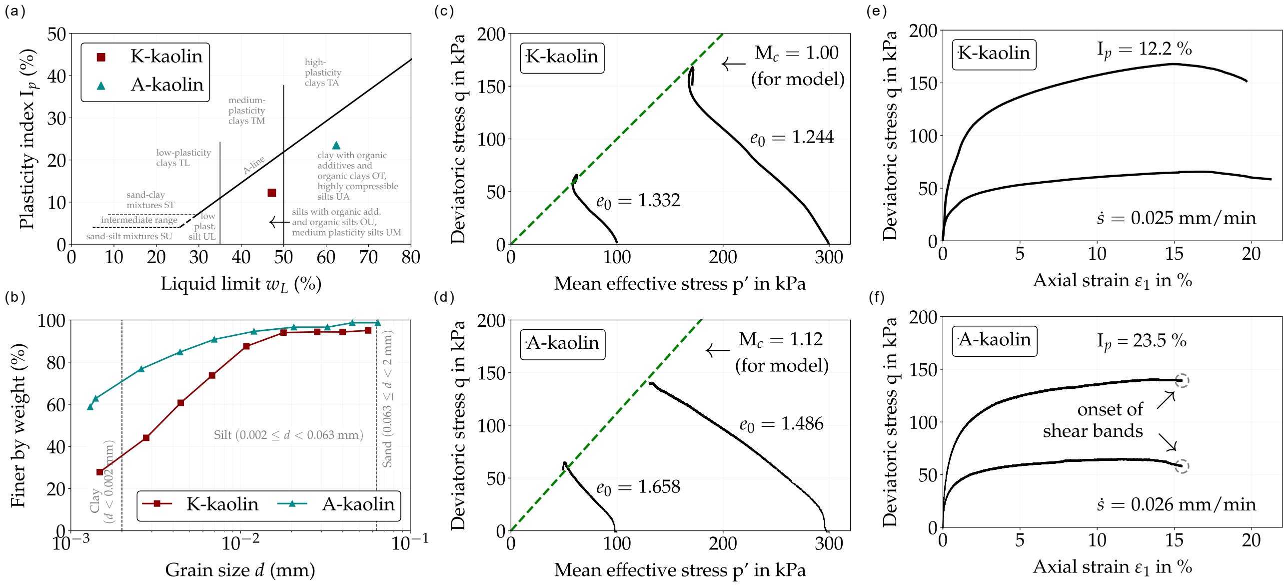

Figure 1. a-b) Position in the plasticity chart (Casagrande's diagram) and GSD curves, c-f) results of CU monotonic tests.

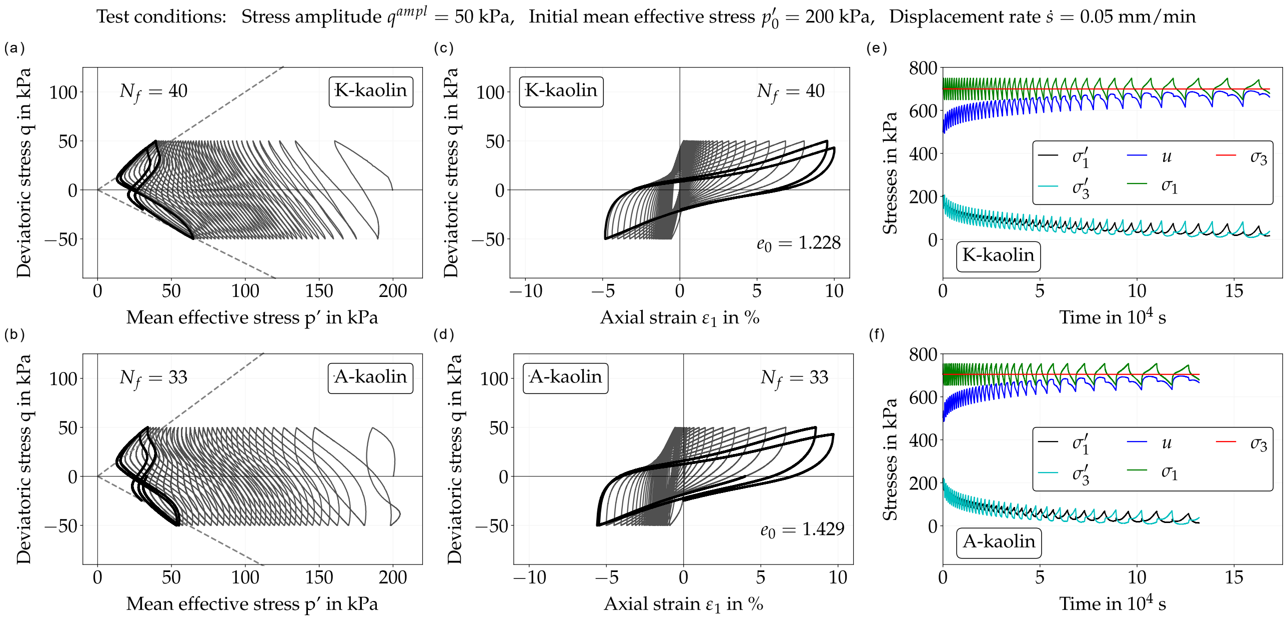

Figure 2. Results of CU cyclic tests: a-b) effective stress path in the $p' - q$ plane, c-d) stress-strain relationship $q(\varepsilon_1)$, e-f) stress components and pore pressure over time.

3 Numerical simulations

In the following section the performance of the anisotropic visco-hypoplastic (AVHP) model proposed by [2], accounting for strain rate dependency and inherent anisotropy, is inspected on the basis of CU cyclic triaxial tests. A starting parameter set for A-kaolin was determined based on CU monotonic triaxial tests for the determination of the critical friction φ_c, the reference strain rate $\dot{\varepsilon}_r$, the reference void ratio e_0 and the viscosity index I_v. As for the latter, a test with changes in the displacement rate was considered. Moreover, the parameters λ and κ were estimated by means of a stress controlled oedometer test with loading and unloading phases. The parameter C_1, used in the definition of the hypoplastic strain, directly influences the cumulative rates under cyclic loading conditions and thus calibrated to match as close as possible the measured curves of accumulated excess pore pressure. Lastly, the parameters C_2 and C_3 are responsible for the evolution and limiting effects of anisotropy within the model. These last parameters were determined based on values reported in the literature. The parameter sets for the AVHP model considered in the simulations are given in Table 2.

Table 2. Parameters of the anisotropic visco-hypoplastic (AVHP) model adopted for K-kaolin [a] and A-kaolin.

Material	φ_c	$\dot{\varepsilon}_r$	e_0 [b]	λ	κ	I_v	C_1	C_2	C_3
K-kaolin [a]	25.4 °	10^{-6} (1/s)	1.125	0.046	0.036	0.014	Variable	600	0.645
A-kaolin	28.1 °	$3.3\cdot10^{-6}$ (1/s)	1.625	0.1	0.029	0.017		600	0.367

[a] From Wichtmann [3], [b] Reference void ratio at $p_0 = 100$ kPa.

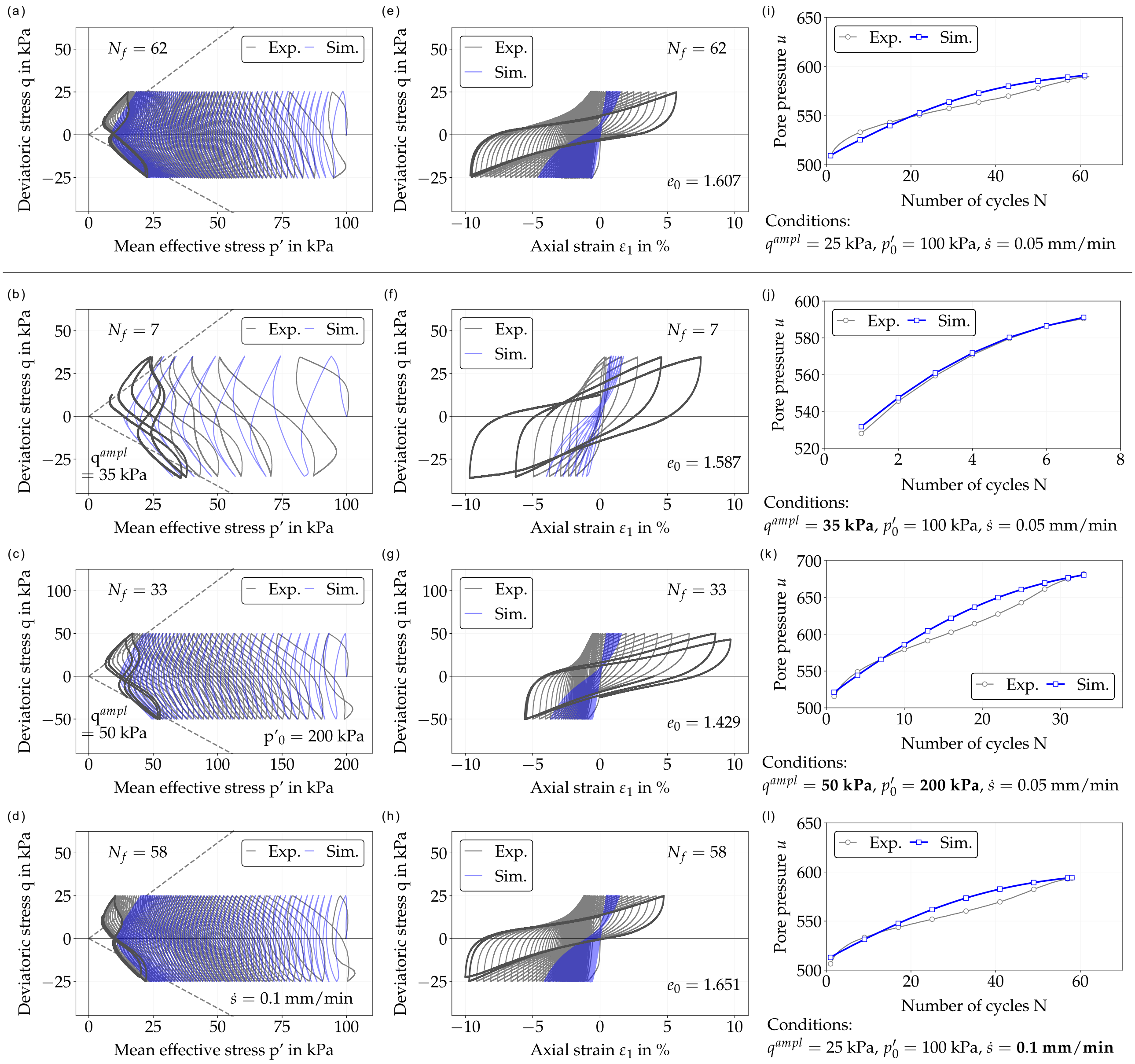

Figure 3. Comparison between experimental results of CU cyclic tests and simulations with the AVHP model for A-kaolin: a-d) effective stress path in the $p' - q$ plane, e-h) stress-strain relationship $q(\varepsilon_1)$, i-l) pore pressure evolution vs. the number of cycles.

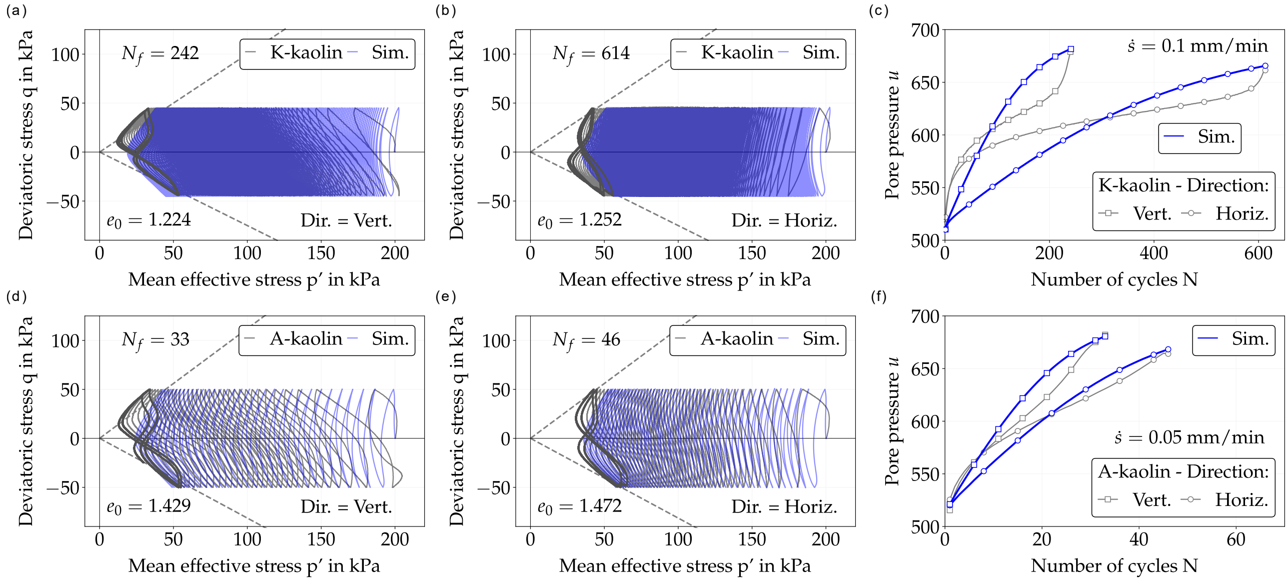

Figure 4. Comparison between experimental results of CU cyclic tests with samples cut out in the horizontal or vertical direction and simulations with the AVHP model. For: a-c) K-kaolin, d-f) A-kaolin.

Although the evolution of pore pressure u is reproduced reasonably well, see Figures 3i-l, the simulated stress-strain loops exhibit a higher slope compared to the experimental results, leading to a lower axial strain accumulation than in the experiment. This can be partly explained by the independent control of the magnitude of the stress relaxation (rate of pore pressure accumulation) by means of a single parameter C_1. Notably, the AVHP model is not capable of reproducing the final eight-shaped effective stress path loops shown in the experiments. To inspect the influence of inherent anisotropy, selected tests with samples extruded from preconsolidated blocks in the horizontal direction, i.e., rotation of 90°, are compared in Figure 4. Similarly, as observed for K-kaolin, the results on A-kaolin show a significant effect on anisotropy demonstrated in the change in inclination of the effective stress path and a higher stiffness leading to a larger number of cycles to failure N_f for the samples cut in the horizontal direction.

4 Summary and outlook

An experimental investigation of Eckalite-1 Australian kaolin clay (A-kaolin), comprising undrained triaxial tests under monotonic and cyclic loading was carried out. Based on the comparison of selected tests with different displacement rates, the effect of the loading rate on the cumulative effects seems to be less significant than initially anticipated, and therefore similar in comparison to the lower plasticity Karlsruhe kaolin clay (K-kaolin). Future work will consider both additional tests under different conditions and further variations of the current experiments to validate the hereby derived observations. In addition, the current experimental results were used to derive an initial set of parameters of the anisotropic visco-hypoplastic (AVHP) model for A-kaolin. Based on the element test simulations for both A-kaolin and K-kaolin, the ability of the model to capture key features of the material behaviour was inspected with focus on cyclic loading. In this sense, the model predicted an overestimation of the soil stiffness as observed in the stress-strain relationships $q(\varepsilon_1)$, while reproducing satisfactorily the evolution of pore pressure u. In view of this, the formulation and calibration of the model, e.g., the C_1 parameter controlling the cumulative rate, needs further inspection. Additionally, coupling of the AVHP model with paraelasticity [4] is planned in order to incorporate small strain effects.

The authors are grateful for the financial support provided by the German Research Council (DFG) - project No.: 409759834.

References

1. T. Wichtmann and T. Triantafyllidis, Monotonic and cyclic tests on kaolin: a database for the development, calibration and verification of constitutive models for cohesive soils with focus to cyclic loading. Acta Geotech., **13**, 1103-1128 (2018). https://doi.org/10.1007/s11440-017-0588-3
2. A. Niemunis, C.E. Grandas-Tavera and L. F. Prada-Sarmiento, Anisotropic visco-hypoplasticity. Acta Geotech., **4**, 293-314 (2009). https://doi.org/10.1007/s11440-009-0106-3
3. T. Wichtmann, Soil behaviour under cyclic loading - experimental observations, constitutive description and applications. Habilitation, Karlsruher Institut für Technologie (KIT) (2016).
4. L. F. Prada-Sarmiento, Paraelastic description of small-strain soil behaviour. PhD thesis, Karlsruher Institut für Technologie (KIT) (2011).